Organic & Biomolecular Chemistry

Accepted Manuscript

ROYAL SOCIETY OF CHEMISTRY

www.rsc.org/obc

Binding of pixantrone to DNA at CpA dinucleotide sequences and bulge structures

Shyam K. Konda[a], Haiqiang Wang[a], Suzanne M. Cutts[b*],
Don R. Phillips[b] and J. Grant Collins[a*]

[a] School of Physical, Environmental and Mathematical Sciences
University of New South Wales
Australian Defence Force Academy
Northcott Drive, Campbell, ACT 2600
Australia
Email: g.collins@adfa.edu.au

[b] Biochemistry Department
La Trobe University
Bundoora, VIC, 3083
Australia
Email: s.cutts@latrobe.edu.au

Please address editorial correspondence to Professor Grant Collins
E-mail: g.collins@adfa.edu.au

Graphical Abstract

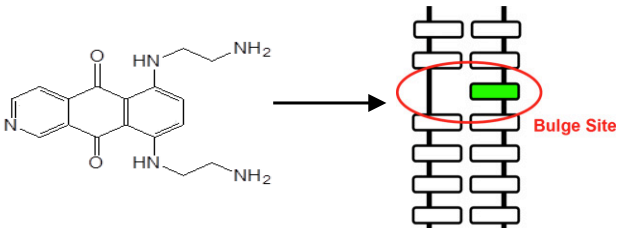

The anti-cancer drug pixantrone intercalates predominantly from the minor groove at adenine bulge sites, but with approximately equal frequency from the minor and major grooves at CpA sites.

Abstract

The binding of the anti-cancer drug pixantrone to three oligonucleotide sequences, d(TCATATGA)$_2$, d(CCGAGAATTCCGG)$_2$ {double bulge = DB} and the non-self complementary d(TACGATGAGTA):d(TACCATCGTA) {single bulge = SB}, has been studied by NMR spectroscopy and molecular modelling. The upfield shifts observed for the aromatic resonances of pixantrone upon addition of the drug to each oligonucleotide confirmed the drug bound by intercalation. For the duplex sequence d(TCATATGA)$_2$, NOEs were observed from the pixantrone aromatic H7/8 and aliphatic Ha/Hb protons to the H6/H8 and H1' protons of the C_2, A_3, T_6 and G_7 nucleotides, demonstrating that pixantrone preferentially binds at the symmetric CpA sites. However, weaker NOEs observed to various protons from the T_4 and A_5 residues indicated alternative minor binding sites. NOEs from the H7/H8 and Ha/Hb protons to both major (H6/H8) and minor groove (H1') protons indicated approximately equal proportions of intercalation was from the major and minor groove at the CpA sites. Intermolecular NOEs were observed between the H7/H8 and H4 protons of pixantrone and the A_4H1' and G_3H1' protons of the oligonucleotide that contains two symmetrically related bulge sites (DB), indicative of binding at the adenine bulge sites. For the oligonucleotide that only contains a single bulge site (SB), NOEs were observed from pixantrone protons to the SB G_7H1', A_8H1' and G_9H1' protons, confirming that the drug bound selectively at the adenine bulge site. A molecular model of pixantrone-bound SB could be constructed with the drug bound from the minor groove at the A_8pG_9 site that was consistent with the observed NMR data. The results demonstrate that pixantrone preferentially intercalates at adenine bulge sites, compared to duplex DNA, and predominantly from the minor groove.

Introduction

Pixantrone {6,9-bis[(2-aminoethyl)amino]benzo[*g*]isoquinoline-5,10-dione dimaleate - see Figure 1} is an aza-anthracenedione anti-neoplastic drug that is related to the well known anthracycline class of drugs.[1-4] Unlike the parent anthracyclines that exhibit irreversible and cumulative cardiotoxicity,[5] pixantrone was designed to reduce the treatment-related cardiotoxicity while retaining efficacy.[1,2] Pixantrone shows activity against a range of cancers, with excellent potential for the treatment of haematological malignancies, particularly lymphomas and leukaemia.[1,2] Pixantrone passed Phase II clinical trials for the treatment of non-Hodgkin's lymphoma,[3] and has recently been shown to be efficacious and tolerable in Phase III studies.[4]

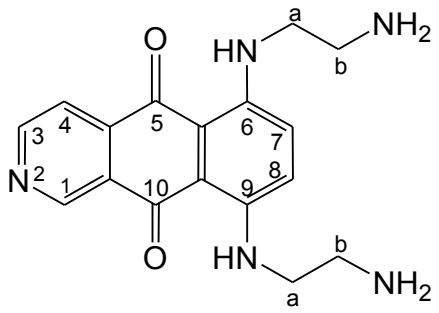

Figure 1. Structure and atom numbering of pixantrone.

Due to its extended electron-deficient planar aromatic ring system, pixantrone can bind DNA by intercalation and poison topoisomerase II, inhibiting the topological modification of DNA.[6-8] More recently, it has also been demonstrated that pixantrone can be activated by formaldehyde to generate pixantrone-DNA covalent adducts.[9-11] *In vitro* transcriptional analysis established that formaldehyde-activated pixantrone can form covalent adducts selectively at CpG and CpA dinucleotide sites.[10] It has been proposed that these adducts are formed between the primary amino group from

one side chain of pixantrone, activated by formaldehyde, and the exocyclic N-2 of a guanine residue at the CpG or CpA intercalation site.[10]

As the formaldehyde-activated covalent adducts are formed at the N-2 of guanine, it would be expected that covalent bond formation would be favoured by minor groove intercalation which positions the pixantrone aliphatic side-chains near the guanine N-2. However, a recent NMR study demonstrated that pixantrone predominantly bound by intercalation at the CpG site of the octanucleotide $d(ACGATCGT)_2$ from the major groove.[12] Nevertheless, observation of weak NOEs from the methylene side chain protons to various oligonucleotide minor groove protons suggested that a small proportion of the pixantrone also bound in the minor groove. This suggests that the differences in the free energy of binding between the major and minor grooves at CpG sites must be relatively small, and consequently, the proportion of minor groove binding could be significantly altered at other sequences or structures. As transcription studies have demonstrated that formaldehyde-activated pixantrone forms covalent adducts as frequently at CpA as CpG sites,[10] it was of interest to examine the reversible binding of pixantrone at a CpA site.

In addition, it was of interest to establish if intercalation at a "non-standard" DNA structure could modulate the proportion of major groove versus minor groove binding. One such deviation from canonical duplex DNA are unpaired nucleotides referred to as bulges,[13-15] where one strand of the hydrogen-bonded duplex possesses one or more nucleotides which have no counterpart on the opposing strand. Bulges are generally less stable than the analogous sequence composed of normal Watson-Crick base pairs,[13] and can vary in size from a single unpaired nucleotide up to a run of several residues.[13-15] Bulged nucleotides can adopt either an intra-helical or an extra-helical arrangement.[13,15] Although there have been no reported examples of

pixantrone binding at DNA bulge sequences, it has been demonstrated that intercalators in general might preferentially bind at bulge sites.[16-18]

In this study we have examined the DNA binding of pixantrone to three oligonucleotide sequences, d(TCATATGA)$_2$, d(CCGAGAATTCCGG)$_2$ {DB}, and the non-self complementary duplex d(TACGATGAGTA):d(TACCATCGTA) {SB}. The first sequence contains two symmetrically related CpA sites, the second oligonucleotide contains two symmetrically related adenine bulge sites that are both adjacent to a CpG site, while the third sequence contains a single adenine bulge site and a non-adjacent CpG site (see Figure 2).

DB: 5'- C_1 C_2 G_3 A_4 G_5 A_6 A_7 T_8 T_9 C_{10} – C_{11} G_{12} G_{13}
3'- G_{13} G_{12} C_{11} – C_{10} T_9 T_8 A_7 A_6 G_5 A_4 G_3 C_2 C_1

SB: 5'- T_1 A_2 C_3 G_4 A_5 T_6 G_7 A_8 G_9 T_{10} A_{11}
3'- A_{21} T_{20} G_{19} C_{18} T_{17} A_{16} C_{15} – C_{14} A_{13} T_{12}

Figure 2. Sequence and nucleotide numbering for the adenine bulge containing oligonucleotides DB and SB. The adenine bulge residues are indicated in red, as is the CpG site in SB. The CpG site in DB is adjacent to the A_4 residue.

Experimental

Materials

The oligonucleotides were obtained from GeneWorks, South Australia. D_2O (99.9% and 99.6% D) was obtained from Aldrich, and CM-Sephadex from Amersham-Pharmacia-Biotech. Acetonitrile and methanol were obtained from Aldrich chemical

company. All aqueous solutions for the sample preparation and NMR studies were made up in de-ionised Milli-Q water (Cross-Section Millipak-40 Filter Unit, Millipore S.A., France). Pixantrone (BBR 2778) was obtained from Cell Therapeutics Europe, Bresso, Italy.

Sample preparation for NMR analysis

Minor impurities were removed from the oligonucleotides using a reverse-phase Water C18 Sep-Pak cartridge. The cartridge was activated with methanol (10 mL) and then washed with water (2 × 10 mL) before the oligonucleotide solution was loaded. The column was washed with water (2 × 3 mL) and then the oligonucleotide eluted with 50% v/v acetonitrile/water. Fractions of approximately 3 mL each were collected and those fractions containing the oligonucleotide (determined by UV-Vis spectroscopy) were freeze-dried.

The oligonucleotides were then converted from a triethylammonium salt to a sodium salt using a CM-Sephadex column that had been equilibrated with 1 M NaCl. After elution from the column, 650 µL of phosphate buffer (10 mM, pH 7.0) containing 20 mM NaCl and 1 mM EDTA was added and the solution freeze-dried. The oligonucleotide samples were freeze-dried several times from D_2O and finally, dissolved in 650 µL 99.96% D_2O prior to use. The concentration of the oligonucleotide duplex was estimated from the A_{260} absorbance, using an extinction coefficient of 6,600 $M^{-1}cm^{-1}$ per nucleotide. For the non-self complementary oligonucleotide SB, the duplex was obtained by titrating d(TACGATGAGTA) directly into the complementary strand dissolved in the phosphate buffer with the progress monitored by ^1H NMR until a complete reduction of the peaks assigned to d(TACCATCGTA) was observed. For all oligonucleotides, the final duplex samples

were heated to 90 ^{o}C and then left to slowly cool. NMR spectra were then re-acquired in order to confirm that the oligonucleotide samples had achieved the most stable duplex conformation.

NMR spectroscopy

^{1}H NMR spectra were recorded on a Varian Unity*plus*-400 or Bruker DRX-800 spectrometer operating at 400 and 800 MHz, respectively, at 25 ^{o}C unless otherwise stated and the data processed using the Agilent software Vnmrj 2.2C. Chemical shift values were referenced to HDO at 4.78 ppm relative to 2,2-dimethylsilapentane-5-sulfonic acid. NOESY and DQFCOSY spectra were acquired with the HDO resonance suppressed using the Wet pulse sequence using low power selective irradiation with a relaxation delay of 1.7 seconds. A spectral width of 4000 or 8000 Hz, at 400 and 800 MHz respectively, were used with each FID acquired over 2048 points in t_2 for 256 t_1 increments with a mixing time for NOESY spectra ranging from 100 to 300 ms. All data sets were processed with a shifted sinebell or a mild Gaussian function.

Molecular Modelling

The molecular modelling of the free and pixantrone-bound oligonucleotides was carried out using HyperChem Release 7.5 software as previously described.[12,19] Duplex B-DNA was generated from the nucleic acid database. Single-stranded B-type DNA was used to insert the unpaired adenines, with the two segments of the non-bulge containing strand that spanned the bulge site being covalently joined. The unpaired adenine bases were stacked within the duplex. Energy restraints were added to preserve the H-bonds expected of duplex DNA during the optimisation procedures.

The duplex DNA was optimised *in vacuo* by applying the Amber 99 forcefield and a Polak-Ribiere conjugant algorithm with a 5×10^{-5} kcal/(Å mol) convergence criterion. The pixantrone atom charges were determined using the AM1 semi-empirical method. Pixantrone was manually docked at the oligonucleotide binding site based on the observed NOE data. Energy restraints were applied to maintain these close contacts during the AMBER 99 molecular mechanics optimisation process and then removed to confirm the optimised structure was energy minimised.

Results

Pixantrone binding to d(TCATATGA)$_2$

The resonances in the ^{1}H NMR spectra of the free and pixantrone-bound octanucleotide were assigned by standard techniques.[20-22] Although the octanucleotide is less than one complete turn of the helix, analysis of short mixing-time NOESY and DQFCOSY spectra indicated that d(TCATATGA)$_2$ adopted a B-type conformation in the aqueous buffer, consistent with many NMR studies of oligonucleotides.[20-22] While the terminal residues do not form a stable base pair ("end fraying"), the binding mode of pixantrone at the internal CpA site will not be significantly influenced by end fraying. The ^{1}H NMR resonances of free pixantrone have been previously assigned.[12]

Titration of the DNA duplex with pixantrone at 15 °C (see Figure 3), 25 °C and 30 °C (see Figure 4) induced significant broadening of the resonances from both the drug and octanucleotide, indicating that pixantrone binds with intermediate exchange kinetics (on the NMR time scale). Intermediate exchange kinetics is consistent with relatively strong binding by the drug. Due to the extensive broadening of the resonances at either 15 or 25 °C, the resonances from the pixantrone-bound

octanucleotide were assigned from NOESY and DQFCOSY spectra at 30 °C. While the octanucleotide base H8/H6 resonances only exhibited small changes in chemical shift upon pixantrone binding, the resonances from the aromatic protons of the drug shifted significantly upfield (0.54 to 0.87 ppm, see Table 1), consistent with pixantrone binding by intercalation. In addition, the resonances from the aliphatic ethylene side-chain protons shifted upfield to a lesser extent (0.41 and 0.08 ppm) upon addition to the octanucleotide.

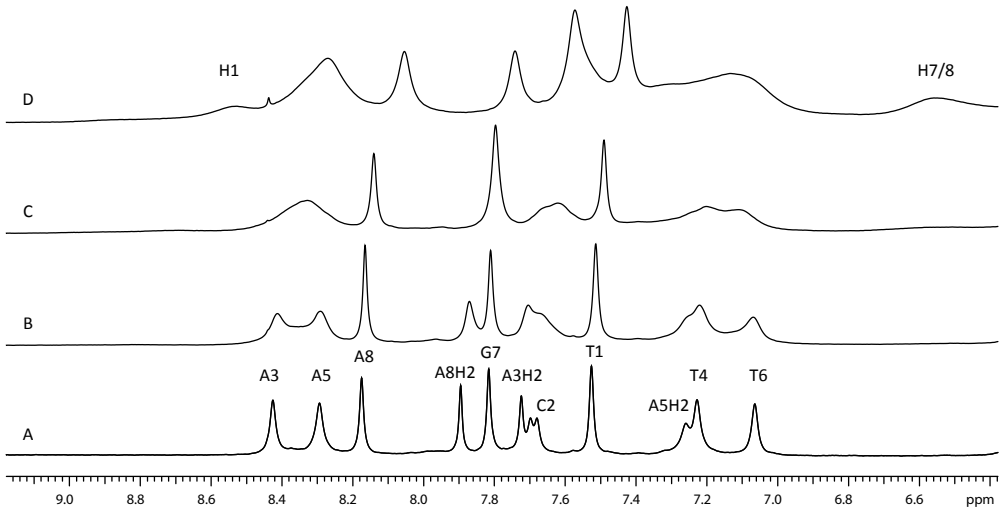

Figure 3. Aromatic region of the ^{1}H NMR spectrum of d(TCATATGA)$_2$ (A) and with added pixantrone, at a drug to duplex ratio of 0.4 (B), 1 (C) and 2 (D) at 15 °C. The H8 and H6 protons of the octanucleotide and H1 and H7/H8 protons of the bound pixantrone are indicated.

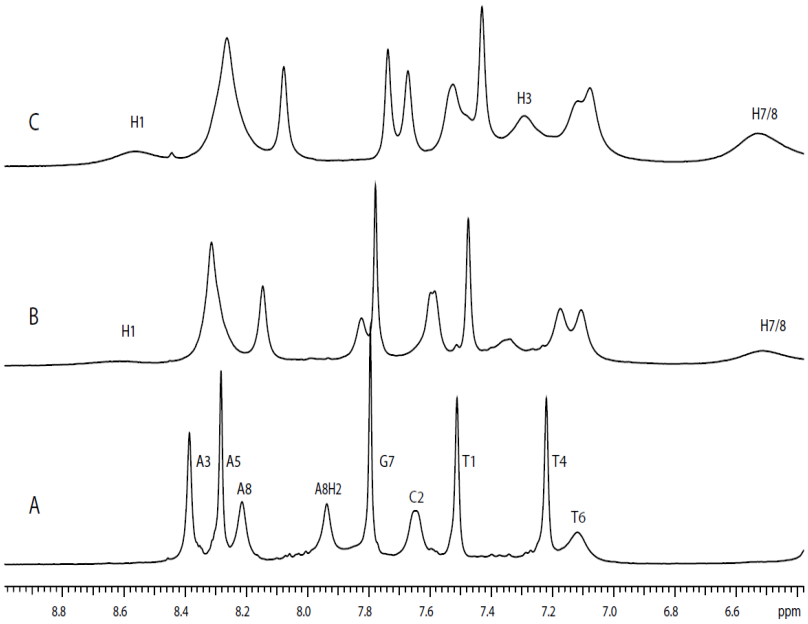

Figure 4. Aromatic region of the ^{1}H NMR spectrum of d(TCATATGA)$_2$ (A) and with added pixantrone, at a drug to duplex ratio of 1.0 (B) and 2 (C) at 30 °C. The H8 and H6 protons of the octanucleotide and the H1, H3 and H7/H8 protons of the bound pixantrone are indicated.

Table 1. ^{1}H NMR chemical shift of pixantrone and pixantrone bound to d(TCATATGA)$_2$, at R = 1 and 2 at 30 °C, in D_2O (pixantrone) and pH 7 phosphate buffer. Changes in chemical shifts are given in brackets, with a negative sign indicating an upfield shift.

Pixantrone	**H1**	**H3**	**H4**	**H7/8**	**Ha**	**Hb**
Free	9.27	8.01	8.85	7.39	3.86	3.35
d(TCATATGA)$_2$ bound, R = 1	8.64 (-0.63)	7.34 (-0.67)	8.31 (-0.54)	6.52 (-0.87)	3.49 (-0.37)	3.31 (-0.04)
d(TCATATGA)$_2$ bound, R = 2	8.60 (-0.67)	7.31 (-0.70)	8.27 (-0.58)	6.54 (-0.85)	3.45 (-0.41)	3.27 (-0.08)

Potentially, the pixantrone binding site could be identified by the observation of significant changes in the chemical shifts of resonances from particular nucleotide

residues within the oligonucleotide. However, no selective pattern of shifts was observed, with at least one resonance from each nucleotide shifting by ≥ 0.1 ppm (see Table 2). Consequently, NOESY spectra were recorded to obtain a detailed picture of the pixantrone-octanucleotide binding. Intermolecular NOEs of intermediate strength were observed between protons from pixantrone and the octanucleotide. In particular, NOEs were observed from the pixantrone aromatic H7/8 and aliphatic Ha/Hb protons to the H6/H8 and H1' protons of the C_2, A_3, T_6 and G_7 nucleotides of the octanucleotide (see Figures 5 and 6). These intermolecular NOEs indicate that pixantrone does preferentially bind at the symmetric CpA sites in the octanucleotide, as expected. However, weaker NOEs observed to various protons from the T_4 and A_5 residues indicate alternative minor binding sites.

Table 2. ^{1}H NMR assignment of the DNA resonance of d(TCATATGA)$_2$ with added pixantrone at R= 2 in pH 7 phosphate buffer at 30 °C. Changes in chemical shift upon pixantrone binding are given in brackets, with a negative sign indicating an upfield shift.

DNA	H8/H6	H5/H2	H1'	H2'	H2"	Methyl
T_1	7.45 (-0.07)		5.98 (-0.13)	2.07 (-0.12)	2.46 (-0.03)	1.61 (-0.14)
C_2	7.54 (-0.09)	5.65 (-0.26)	5.65 (-0.04)	2.18 (-0.02)	2.40 (-0.03)	
A_3	8.28 (-0.10)	ND	6.16 (-0.13)	2.69 (-0.09)	2.83 (-0.14)	
T_4	7.14 (-0.08)		5.77 (-0.02)	2.17 (0.15)	2.34 (-0.06)	1.30 (-0.30)
A_5	8.28 (0.00)	ND	6.12 (-0.10)	2.64 (-0.03)	2.82 (0.03)	
T_6	7.10 (-0.06)		5.66 (-0.13)	1.87 (0.11)	2.19 (0.01)	1.30 (-0.24)
G_7	7.75 (-0.05)		5.52 (-0.16)	2.48 (-0.03)	2.59 (0.08)	
A_8	8.10 (-0.14)	ND	6.21 (-0.14)	2.65 (-0.04)	2.47 (-0.03)	

In theory, pixantrone could intercalate with its aromatic ring system either parallel or perpendicular to the nucleotide base pairs at the binding site. Models were built to examine both possibilities. Orientation of the pixantrone aromatic ring system parallel to the nucleotide base pairs requires the positioning of one aliphatic side-chain in the major groove and one side-chain in the minor groove. Due to steric clashes between pixantrone aromatic protons (particularly the H3 and H4) and the octanucleotide H2' and H2" protons at the intercalation site, it was not possible to obtain an energy minimised model with the pixantrone aromatic ring system fully parallel with the octanucleotide base pairs. In addition, in the energy minimised models where the pixantrone aromatic rings were slightly rotated from being parallel, the distances from the pixantrone H3 and H7/H8 protons to the octanucleotide H2' and H2" protons were 2.8 to 3.4 Å. As no intermolecular NOEs were observed from the pixantrone H3 and H7/H8 protons to the octanucleotide H2' and H2" protons (see Figure 5), the parallel binding model was discounted. Models were then constructed where the pixantrone aromatic ring system was oriented perpendicular to the nucleotide base pairs. As pixantrone can only intercalate with the heteroaromatic ring as the leading edge, the NOEs from the H7/H8 and Ha/Hb protons to both major (H6/H8) and minor groove (H1') octanucleotide protons indicate approximately equal proportions of intercalation from the major and minor groove. Inter-atomic distance determination from molecular models demonstrate that the H7/H8 and Ha/Hb protons are only within NOE distance (5 Å) to the base H6/H8 protons for intercalation from the major groove, and to the H1' protons for intercalation from the minor groove.

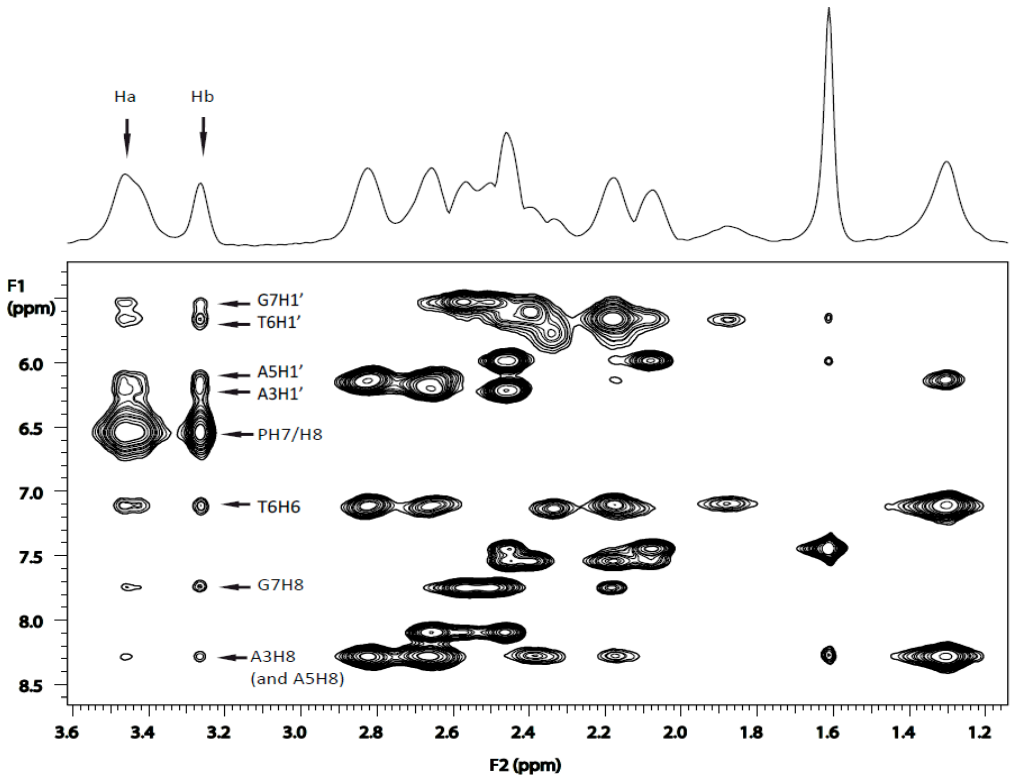

Figure 5. An expansion of a NOESY spectrum of d(TCATATGA)$_2$ with added pixantrone, at a drug to DNA duplex ratio of 2, at 30 °C in D_2O and pH 7 phosphate buffer. The expansion shows the NOE connectivities from the pixantrone Ha and Hb protons (3.27 and 3.45 ppm) to the octanucleotide H8/H6 and sugar H1' protons (8.4 to 5.5 ppm).

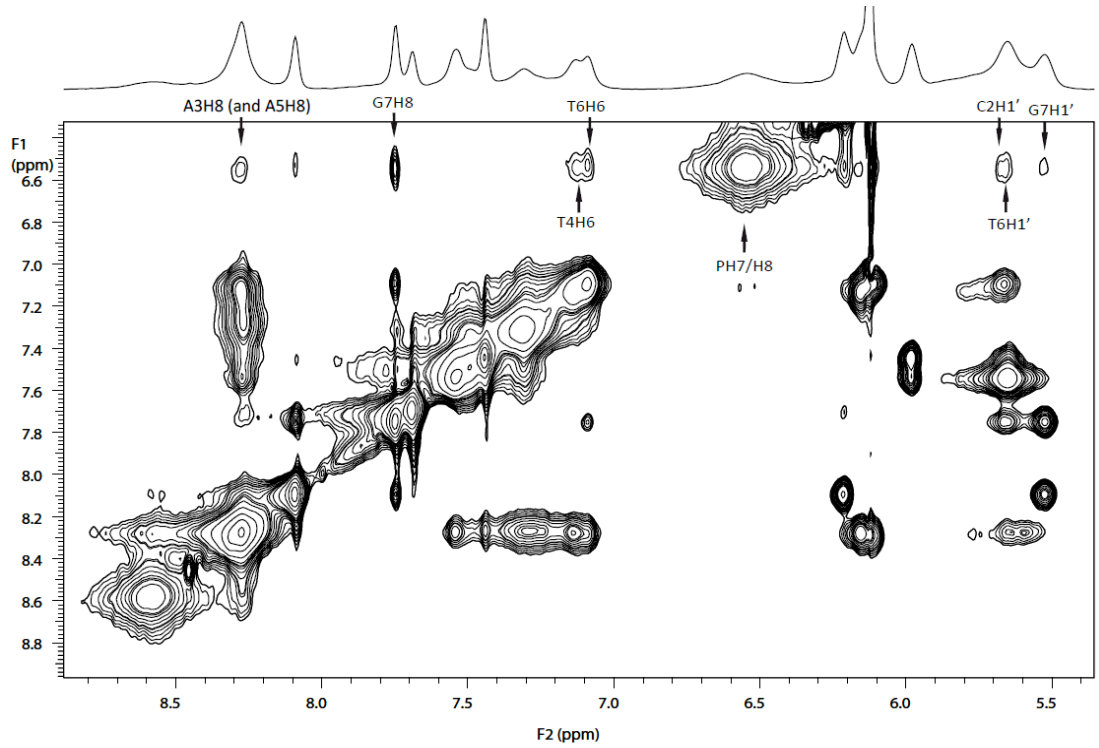

Figure 6. An expansion of a NOESY spectrum of d(TCATATGA)$_2$ with added pixantrone, at a drug to DNA duplex ratio of 2, at 30 °C in D_2O and pH 7 phosphate buffer. The expansion shows the NOE connectivities from the pixantrone H7/H8 protons (6.54 ppm) to the octanucleotide H8/H6 and sugar H1' protons (8.4 to 5.5 ppm).

Pixantrone binding to d(CCGAGAATTCCGG)$_2$ {DB}

The assignment of the ^{1}H NMR resonances of free DB has been previously reported by Kalnik *et al*.,[23] who also established that the duplex adopted a B-type DNA conformation in aqueous solution with the adenine bulge residue stacked within the helix.

As shown in Figure 7, only one set of DB and pixantrone resonances was observed upon addition of the drug to the oligonucleotide at 25 ^{o}C. The aromatic resonances from pixantrone exhibited significant upfield shifts and broadening upon addition to DB, indicating intermediate exchange kinetics (on the NMR time scale).

The upfield shifts of the pixantrone aromatic resonances, summarised in Table 3, is consistent with the drug binding the oligonucleotide by intercalation. At low ratios of added pixantrone, selective broadening of the A_4H8, A_4H2 and $C_{11}H6$ was observed, suggesting that the drug bound at, or adjacent to, the CpG and/or the adenine bulge sites.

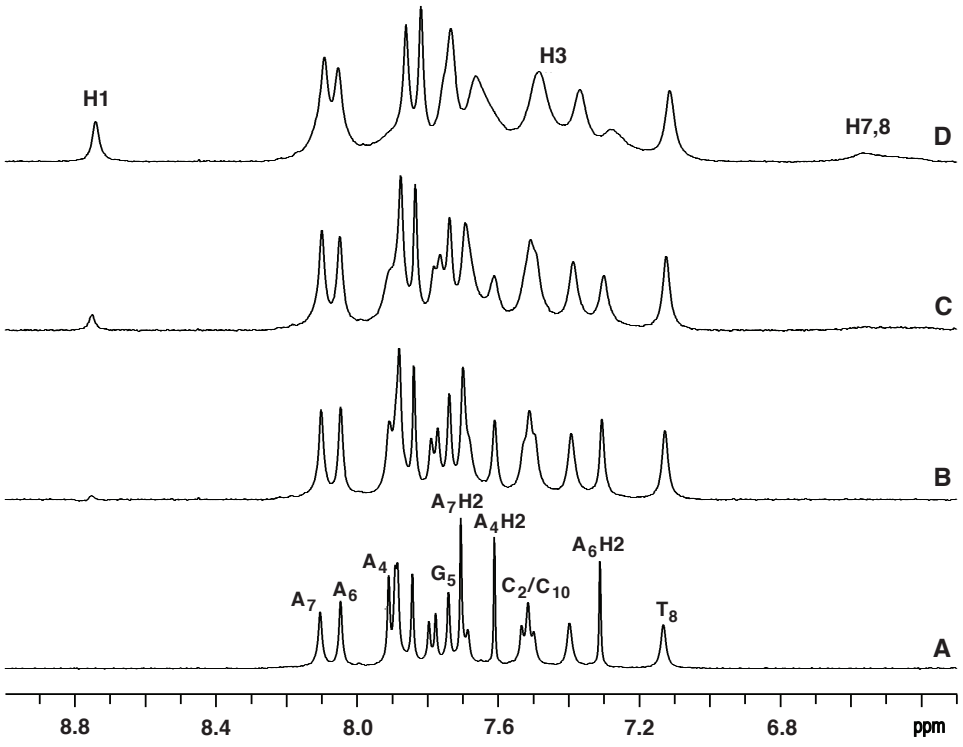

Figure 7. ^{1}H NMR spectrum of free DB (A) and with added pixantrone, at a drug to duplex ratio of 0.25 (B), 0.5 (C) and 1.0 (D), at 25 °C in D_2O and pH 7 phosphate buffer. The assignments of some of the DB base protons are given in spectrum A, while the resonances from the bound pixantrone proton are indicated in spectrum D.

Table 3. Chemical shifts (ppm) of the free pixantrone protons and pixantrone bound to DB, at a ratio (pixantrone to duplex) R = 1 and R = 2 at 25 °C, in D_2O and pH 7 phosphate buffer. Numbers in parentheses indicate the difference between the chemical shift of the bound and free pixantrone protons.

Pixantrone proton	H1	H3	H4	H7/H8	Ha	Hb
Free	9.25	7.99	8.85	7.37	3.85	3.35
DB-bound	8.74	7.50	8.42	6.53	3.76	3.28
R = 1	(-0.51)	(-0.49)	(-0.43)	(-0.84)	(-0.09)	(-0.07)
DB-bound	8.72	7.40	8.38	6.48	3.76	3.26
R = 2	(-0.53)	(-0.59)	(-0.47)	(-0.89)	(-0.09)	(-0.09)

The ^{1}H NMR spectrum of DB with added pixantrone at a drug to oligonucleotide duplex ratio (R) = 1 was recorded as a function of temperature (see Figure 8). Interestingly, at low temperatures multiple resonances were observed for the pixantrone H7/H8 protons. While it could be expected that the chemical shift equivalence of the H7/H8 resonances would be removed upon binding, the observation of four resonances indicates at least two drug-binding sites that are in slow exchange. At 5 ^{o}C, two sets of H7/H8 resonances could be clearly observed, a slightly more intense pair at 6.54 and 6.31 ppm and a smaller set at 6.68 and 6.43 ppm.

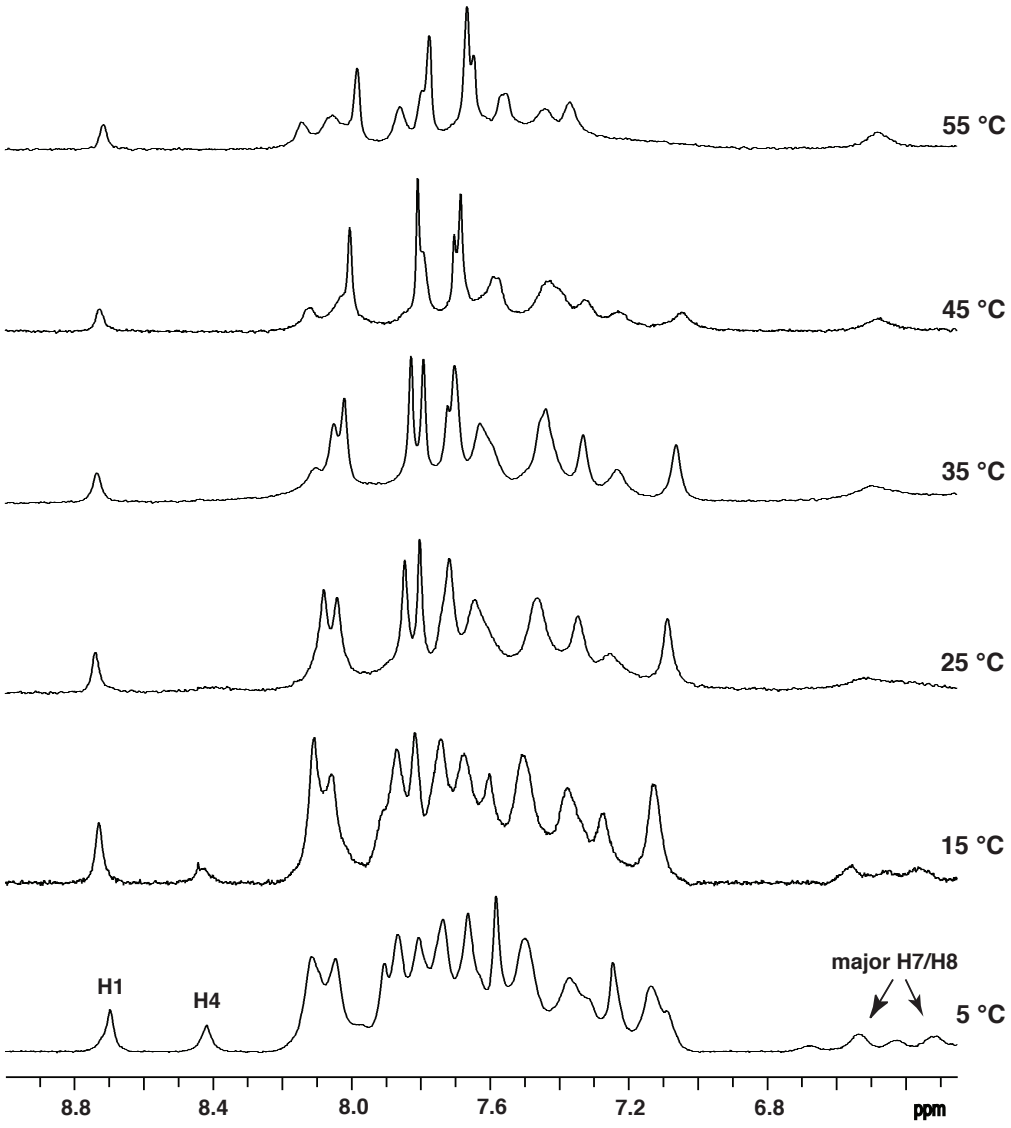

Figure 8. ^{1}H NMR spectrum of DB with added pixantrone, at a drug to duplex ratio of 1.0 in D_2O and pH 7 phosphate buffer as a function of temperature. The H1, H4 and the H7/H8 protons from the major binding form of the bound pixantrone are indicated in the 5 °C spectrum. The H7/H8 resonances from the minor binding form can be seen either side of the resonance at 6.54 ppm.

NOESY spectra were recorded to obtain a more detailed picture of the pixantrone-DB binding. NOEs were observed from the pixantrone H7/H8 and H4 protons to the DB A_4H1' and G_3H1' protons, respectively (see Figure 9). The NOEs from the H7/H8 protons to the minor groove H1' protons indicate binding from the

minor groove, whereas, an NOE from the H4 to the G_3H1' is consistent with intercalation from the major groove. Furthermore, while the NOE between the H4 and the G_3H1' is consistent with major groove intercalation at the preferred duplex binding site, CpG, the NOEs to the A_4H1' are not consistent with this binding. The NOEs between the pixantrone H7/H8 and the DB A_4H1' proton suggests binding at the A_4 bulge site from the minor groove.

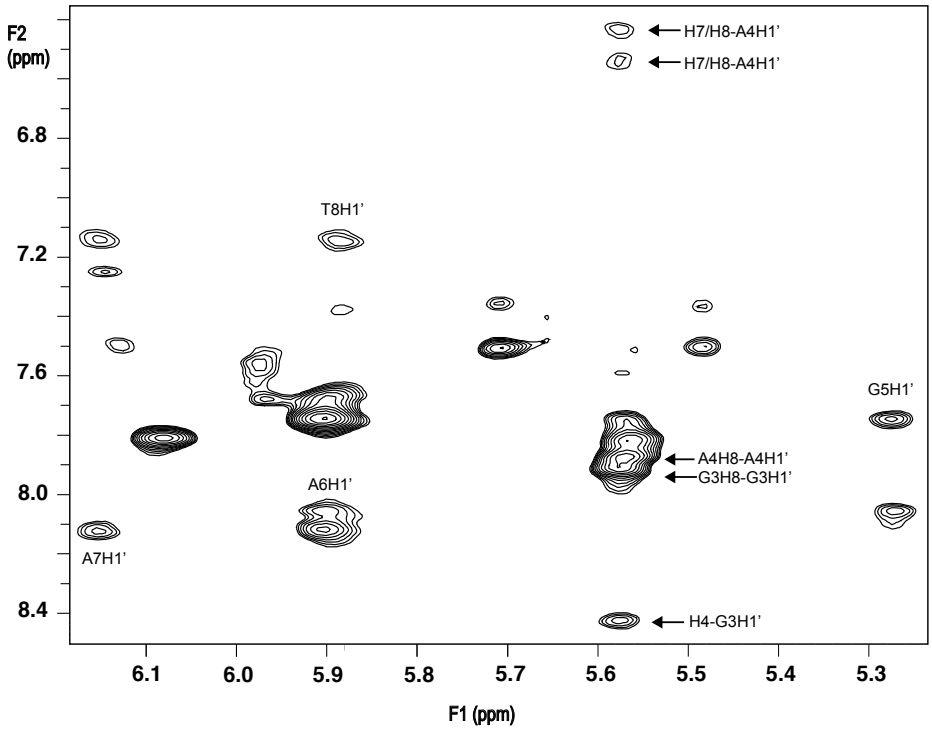

Figure 9. An expansion of a NOESY spectrum of DB with added pixantrone, at a drug to DNA duplex ratio of 1, in pH 7 phosphate buffer at 5 °C. The expansion shows the NOE connectivities from the DB base and pixantrone aromatic protons (6.4 to 8.4 ppm) to the DB sugar H1' protons (5.20 to 6.20 ppm). The NOEs from the H4, H7 and H8 protons of pixantrone to the G_3H1' and A_4H1' of DB are indicated. The unambiguous assignment of the intermolecular NOEs from the pixantrone H4 and H7/H8 protons to the G_3H1' and A_4H1' resonances, respectively, cannot be made from this figure as the G_3H1' and A_4H1' resonances have coincidental chemical shifts. The assignments were

made from the corresponding cross peaks above the diagonal where greater resolution in the sugar H1' resonances (F2 axis) is obtained and the G_3H1' and A_4H1' resonances can be resolved (see Figure S2 in the ESI).

The NMR results are consistent with pixantrone binding DB by intercalation, and the NOEs observed between the pixantrone protons and the DB A_4H1' and G_3H1' protons indicate that the drug intercalates at either or both the CpG site or adjacent bulge site. It is possible that pixantrone could intercalate at the bulge site by "flipping-out" the A_4 base from the helical stack, and thereby, allowing complementary pairing of the nucleotides above and below the intercalated drug. This mode of binding has been previously reported for the binding of nogalamycin with a hairpin oligonucleotide,[24] where the drug stabilised an extra-helical bulged conformation in which a thymine base at the intercalation site was flipped-out of the helix. Large downfield shifts were observed for the base and sugar H1' resonances for the extra-helical thymidine residue.[24] By contrast, the H8 and sugar H1' resonances of A_4 only shifted by 0.01 ppm upon addition of pixantrone to the DB oligonucleotide, and NOEs were observed between the G_5H8 and the A_4H1' protons. Consequently, it was concluded that the A_4 bulge remains within the helical stack. Models were built with pixantrone binding from the major groove at the CpG site, consistent with our previous study,[12] and from the minor groove at the GpA bulge site. Table 4 summarises the measured inter-proton distances obtained from the various models.

Table 4. Inter-proton distances in pixantrone bound to DB models. Model A has the heteroaromatic nitrogen facing towards the strand containing the bulge residue, while model B has the heteroaromatic nitrogen away from the strand containing the bulge residue.

5'-(C_2pG_3) major groove binding			5'-(G_3pA_4) minor groove binding		
pixantrone-oligonucleotide	distance (Å)		pixantrone-oligonucleotide	distance (Å)	
	A	B		A	B
H7-A_4H1'	13.5	10.6	H7-A_4H1'	5.3	4.9
H8-A_4H1'	11.9	11.3	H8-A_4H1'	3.5	6.7
H4-G_3H1'	9.5	4.4	H4-G_3H1'	7.4	3.1

From the data presented in Table 4, it is clear that the observed pattern of NOEs is not consistent with intercalation at the CpG site. Models with pixantrone intercalated from the minor groove at the CpG site were also examined; however, the inter-proton distances H7-A_4H1', H8-A_4H1' and H4-G_3H1' were all greater than 7 Å, that is, beyond the 5 Å maximum distance for which an NOE could be expected. Alternatively, the modelling suggests that intercalation at the GpA bulge site is consistent with all the observed NOEs. However, it is possible that pixantrone is binding at both the CpG and GpA bulge sites, with the H4-G_3H1' NOE due to intercalation from the major groove at the preferred duplex binding site, and the H7/H8-A_4H1' NOEs to binding at the bulge site. Nevertheless, the results of the pixantrone binding to the bulge containing DB indicate the drug can bind at bulge

sites from the minor groove. This is the first study to demonstrate that pixantrone can bind from the minor groove, and the first example of binding to a non-duplex DNA structure.

Pixantrone binding to d(TACGATGAGTA):d(TACCATCGTA) {SB}

In order to more clearly demonstrate the preferential binding of pixantrone at a bulge site, compared to CpG, and confirm intercalation from the minor groove at the bulge site, the binding of pixantrone to SB was examined. Aliquots of a stock solution of pixantrone were titrated directly into a NMR tube containing the SB oligonucleotide. Although the resonances from SB exhibited significant broadening, the base H8/H6/T-methyl and sugar H1', H2' and H2" resonances could be assigned at 2 ^{o}C (see Table 5). The addition of pixantrone did not induce any significant shifts for the aromatic base or sugar protons from SB. Figure 10 shows the spectra of the imino protons for the free and pixantrone-bound SB at 2 ^{o}C. Significant upfield shifts and broadening were observed for the imino resonances from the G_9, G_7 and to a lesser extent G_4. This suggests that pixantrone bound at the bulge site (A_8), and as the upfield shift is larger for G_9, it is likely that the drug is predominantly intercalated at the G_9•C_{14} base pair. A small upfield shift for the G_4 imino resonance indicates some minor intercalative binding at the C_3pG_4 site. As noted with DB, based upon the observed small changes in chemical shifts for the resonances from A_8 upon addition of pixantrone (see Table 5), it was concluded that the A_8 bulge remains in the helical stack.

Table 5. Chemical shift assignments for the free and pixantrone-bound SB at a pixantrone to duplex ratio of 1.0 at 2 °C. Numbers in parentheses indicate the difference between the chemical shift of the bound and free SB. (ND = Not Determined).

Base	H8/H6	AH2	H1'	H2'	H2''	Methyl
T_1	7.34 (0.01)		5.69 (-0.01)	2.14 (-0.03)	2.15 (-0.03)	1.55 (-0.04)
A_2	8.41 (0.00)	7.52 (0.02)	6.25 (-0.01)	2.92 (-0.03)	2.94 (-0.04)	
C_3	7.32 (-0.01)		5.41 (-0.02)	2.32 (-0.04)	2.82 (-0.01)	
G_4	7.89 (0.01)		5.66 (-0.02)	2.00 (-0.04)	2.70 (-0.04)	
A_5	8.23 (-0.01)	7.74 (0.04)	6.17 (-0.01)	2.26 (-0.02)	2.90 (-0.02)	
T_6	7.03 (0.01)		5.65 (-0.02)	2.02 (-0.03)	2.02 (-0.05)	1.39 (-0.04)
G_7	7.83 (0.01)		5.53 (0.00)	2.44 (-0.04)	2.45 (-0.02)	
A_8	8.00 (0.00)	7.89 (ND)	5.66 (-0.01)	2.46 (-0.02)	2.56 (-0.01)	
G_9	7.86 (-0.01)		5.74 (-0.04)	2.59 (-0.03)	2.62 (-0.03)	
T_{10}	7.22 (-0.01)		5.84 (-0.02)	1.92 (0.01)	2.26 (-0.02)	1.41 (-0.04)
A_{11}	8.24 (0.01)	7.64 (0.02)	6.31 (-0.02)	2.43 (-0.03)	2.70 (-0.04)	
T_{12}	7.30 (0.01)		5.71 (0.00)	2.12 (-0.02)	2.13 (-0.02)	1.54 (-0.05)
A_{13}	8.39 (-0.01)	7.90 (ND)	6.25 (-0.02)	2.81 (-0.03)	2.90 (-0.04)	
C_{14}	7.31 (0.01)		6.26 (-0.02)	2.90 (-0.04)	2.91 (-0.03)	
C_{15}	7.73 (0.00)		5.25 (-0.01)	2.28 (-0.02)	2.42 (-0.02)	
A_{16}	8.41 (0.00)	7.73 (0.03)	6.26 (-0.02)	2.78 (-0.03)	2.81 (-0.02)	
T_{17}	7.20 (-0.01)		5.86 (-0.02)	2.03 (-0.04)	2.43 (-0.02)	1.39 (-0.03)
C_{18}	7.42 (0.01)		5.65 (-0.02)	2.01 (-0.03)	2.37 (-0.02)	
G_{19}	7.93 (0.00)		5.88 (-0.02)	2.57 (-0.03)	2.65 (-0.03)	
T_{20}	7.19 (-0.01)		5.80 (-0.01)	1.92 (-0.01)	2.26 (-0.02)	1.53 (-0.04)
A_{21}	8.23 (0.01)		6.29 (-0.02)	2.43 (-0.02)	2.69 (-0.04)	

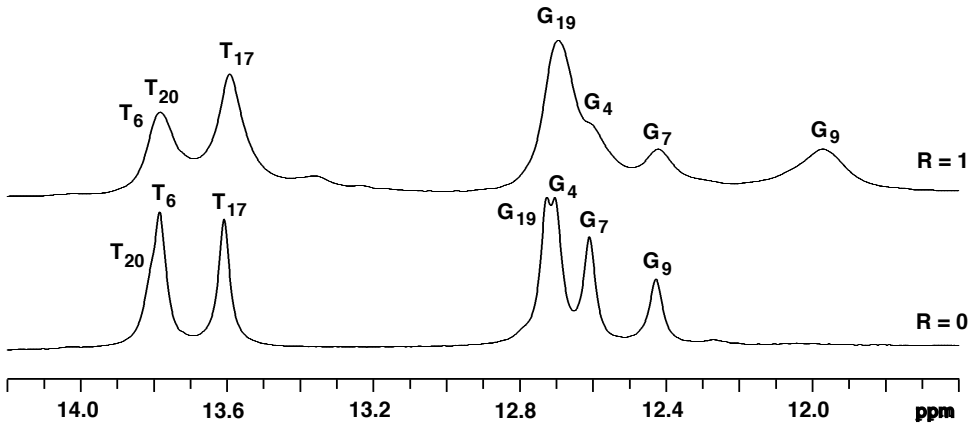

Figure 10. ^{1}H NMR spectra of the imino resonances of SB (R = 0) and with added pixantrone (R = 1), at 2 °C in 90%/10% H_2O/D_2O in pH 7 phosphate buffer.

Figure 11 shows an expansion of the NOESY spectrum of SB with added pixantrone at R = 1. Although some cross peaks were substantially weaker compared to those in the spectrum of the free SB, it was possible to observe an NOE from each base H8/H6 proton to its own and 5'-nucleotide H1', H2' and H2" protons for most of the nucleotides. Of particular note in Figure 11 are the NOEs from the pixantrone H7/H8 protons to the SB A_8H1' proton. Furthermore, no intermolecular NOEs were observed between the pixantrone H7/H8 protons and the minor groove H4', H5' and H5" protons. The absence of an NOE cannot be used as conclusive evidence for a particular binding mode, particularly given the differential broadening of the resonances from SB. However, the sugar H1' protons are located deep within the minor groove, whereas, the H4', H5' and H5" protons are located near the "top" of the groove on the sugar phosphate backbone. Consequently, the NOEs from the pixantrone H7/H8 protons to the SB A_8H1' proton are consistent with intercalation above or below the A_8 nucleotide. Furthermore, NOEs were also observed from the

Ha and Hb side-chain protons of pixantrone to the G_7H1', A_8H1' and G_9H1' protons of SB (see Figure 12). The NOEs to the G_9H1' were stronger than those to the G_7H1', consistent with the larger exchange averaged upfield shift for the G_9 imino resonance upon pixantrone binding.

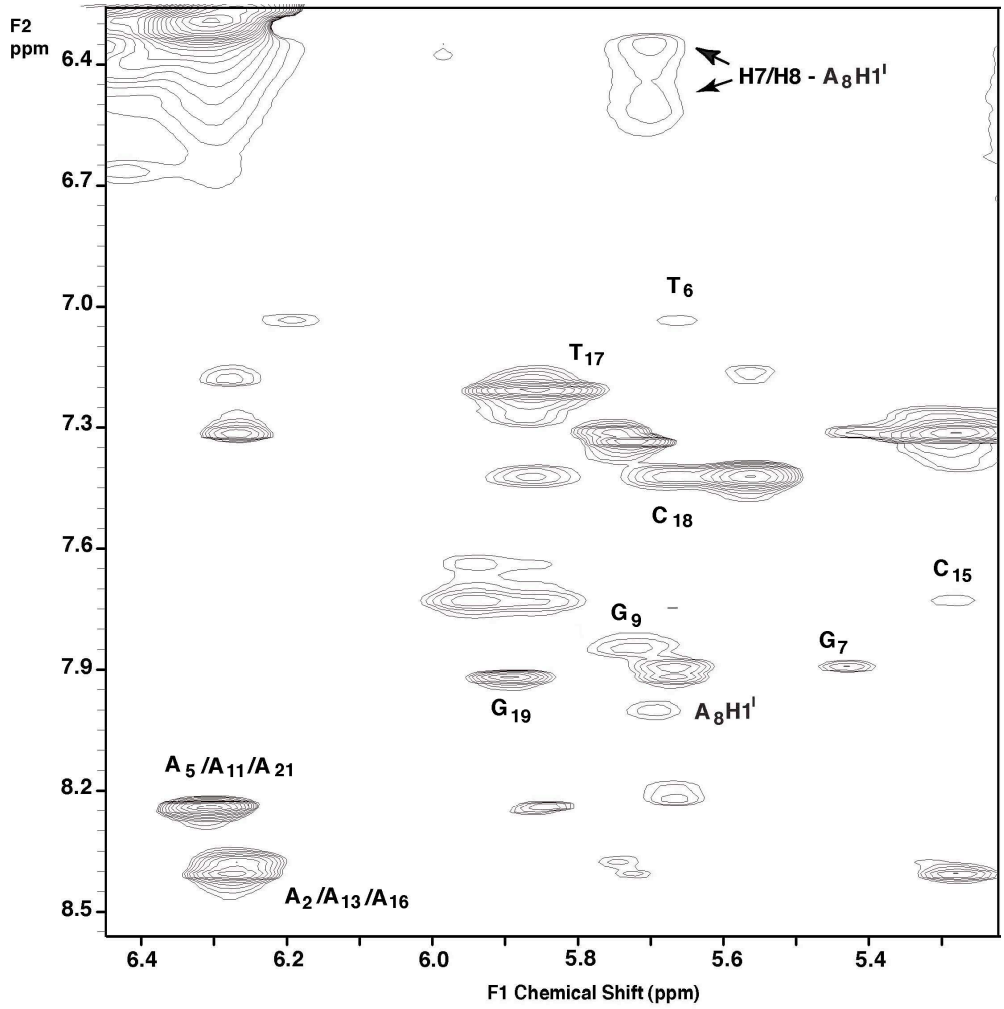

Figure 11. An expansion of a 800 MHz NOESY spectrum of SB with added pixantrone at a drug to SB duplex ratio of 1, in pH 7 phosphate buffer at 5 °C. The expansion shows the NOE connectivities from the SB base and pixantrone aromatic protons (6.4 to 8.5 ppm) to the SB sugar H1' protons (5.20 to 6.40 ppm). NOEs from the H7/H8 protons of pixantrone to the A_8H1' of SB are indicated, as are the sugar H1' protons (e.g. T_6) for most of the SB residues.

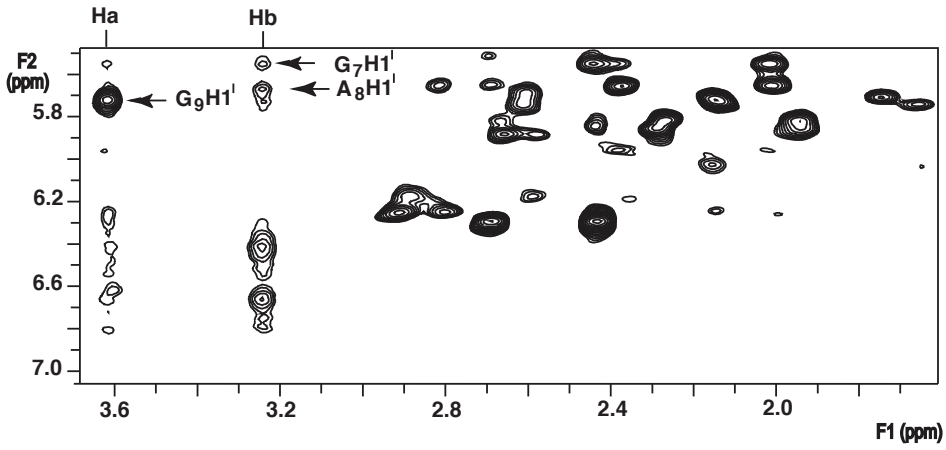

Figure 12. An expansion of a 400 MHz NOESY spectrum of SB with added pixantrone at a drug to duplex ratio of 1, in pH 7 phosphate buffer at 2 °C. The expansion shows the NOEs from the Ha and Hb protons of pixantrone to the G_7H1', A_8H1' and G_9H1' of SB.

Figure 13 shows models of the free and pixantrone-bound SB with the drug binding from the minor groove at the A_8pG_9 site, consistent with the observed intermolecular NOEs from pixantrone to both the A_8H1' and G_9H1'. A close-up of pixantrone bound at the A_8pG_9 site is presented in Figure S3 in the ESI. Pixantrone intercalates between the bulge adenine A_8 and its 3'-guanine G_9 significantly enlarging the distance between A_8 and G_9. The two positively charged side chain amino groups in the minor groove interact with the phosphate backbones. No notable base buckle was found except at the bulge site, consistent with the NOESY experiment results. Additional bending of the duplex was observed at the binding site. There is normally bending at the unbound bulge site, because of the unequal length of the strands. Upon drug intercalation, the bending increased because both strands are stretched to form the intercalation pocket. The long strand stretches easily, while the short strand must twist and bend.

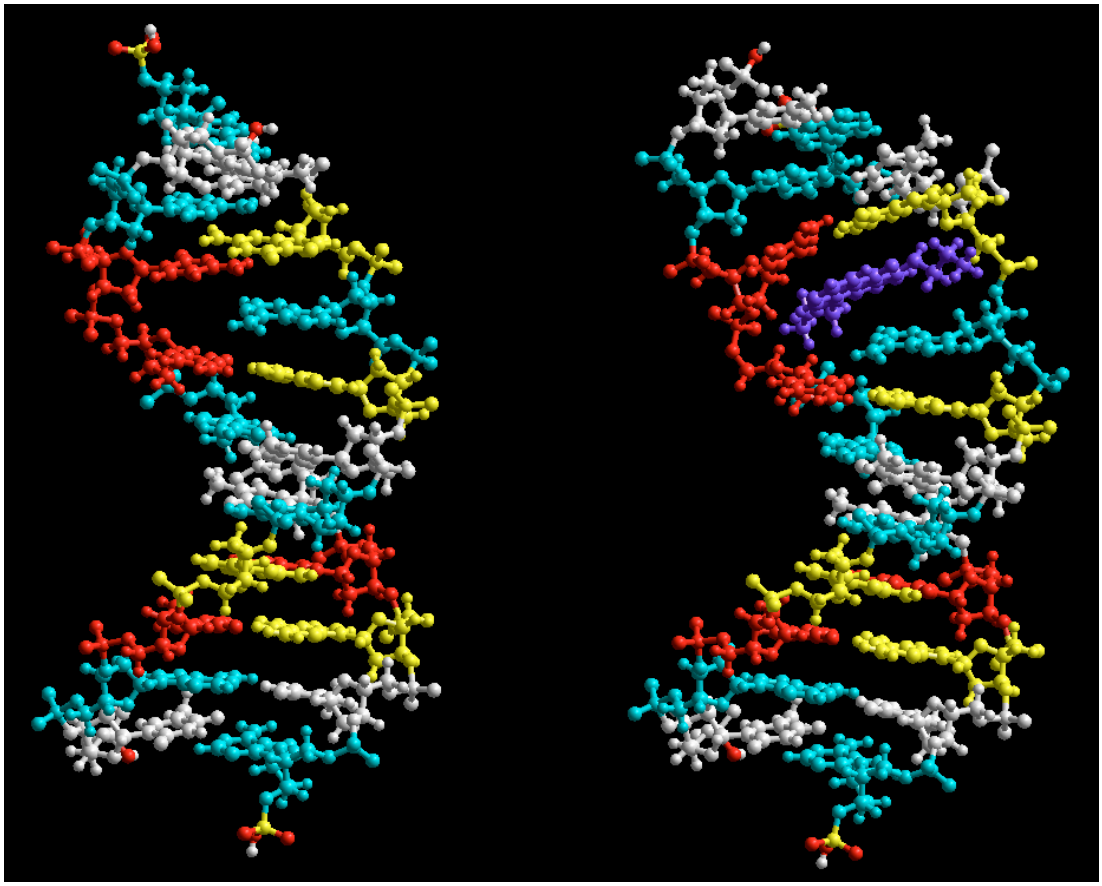

Figure 13. Energy minimised HyperChem molecular models of the free (left-hand side) and pixantrone-bound SB (right-hand side) generated using HyperChem 7.5. The pixantrone is inserted from minor groove at the A_8pG_9 site. The bases are colour coded: adenine (cyan), thymine (white), guanine (yellow) and cytosine (red) and pixantrone is in violet.

Models of pixantrone-bound SB with the drug binding from the minor groove at the G_7pA_8 site were also examined, consistent with the observed intermolecular NOEs from the drug Hb proton to both the G_7H1' and A_8H1' of SB. Similarly to the model with pixantrone intercalated at the A_8pG_9 site, the two positively charged side chain amino groups in the minor groove interact with the phosphate backbones but with the planar ring system stacked under the adenine bulge residue. No significant DNA structural changes beyond the intercalation site were observed.

From the two models of pixantrone-bound SB, the A_8pG_9 site is favoured by comparison with the model of the G_7pA_8 site. However, AMBER 99 does not explicitly handle hydrogen bonding, and the energy difference favouring the A_8pG_9 site is equivalent to two strong hydrogen bond (< 20 kcal/mol). Since both models reveal potential for forming hydrogen bonds, it is only with caution that the A_8pG_9 site can be regarded as energetically favoured by the models. Nevertheless, the stronger pixantrone Ha-G_9H1' and the larger upfield shift of the resonance from the G_9 imino proton suggests that the A_8pG_9 site is the more favoured of the two sites, consistent with the energy comparison between the models.

The models suggest that intercalation at the bulge site is plausible and consistent with the NOESY data, which suggested that intercalation occurs from the minor groove, and can occur either side of the unpaired adenine, and without major perturbation of the overall conformation of the bulged duplex. However, additional conformational features predicted by the models are further widening of the minor groove and further helix bending upon intercalation of bulged helices by pixantrone.

Discussion

The mechanism of anti-cancer activity of pixantrone is yet to be firmly established. While pixantrone can poison topoisomerase II, it does not appear that this mechanism fully accounts for its anti-cancer activity.[7,8] It has also been proposed that pixantrone can be activated by formaldehyde to generate covalent adducts at the N-2 of a guanine, located in the minor groove, at a CpG or CpA site.[10] Furthermore, if the cytosine of a CpG site is methylated at the C-5 position, pixantrone forms 2-5 fold more covalent adducts.[11] Despite the detection of covalent adducts in the DNA minor groove, a previous study has established that pixantrone predominantly (approx. 90%)

intercalates at CpG and ^{Me}CpG sites from the major groove.[12] As the site of covalent binding will be governed to some extent by the initial reversible association with DNA by intercalation, it was of interest to also gain an understanding of the binding mode of pixantrone at CpA sites. Consistent with prior research, the results of this study confirm that pixantrone binds DNA at CpA sites by intercalation. However, it appears that the drug intercalates from either the major or minor groove side of the duplex with approximately equal frequency. A previous study revealed that of the 12 most intense transcriptional blockages induced by formaldehyde-activated pixantrone, 7 involved CpG sites and 5 were at CpA sites.[10] However, of the four most intense blockage sites, three (including the most intense site) were at CpA dinucleotide sites. The results of this study provide one explanation for the observed selectivity for the transcriptional blockages induced by formaldehyde-activated pixantrone.

This study also demonstrates that pixantrone binds more favourably at bulge sites than at CpG sites, and interestingly, from the DNA minor groove. The preferential binding at the bulge site might be explained by the relatively lower free energy cost of forming an intercalation pocket at the bulge site, compared to at a normal base paired duplex site. It is known that bulge sites destabilise the helix,[13] and this was confirmed by the observation of selectively broadened resonances from imino protons adjacent to the bulge site in the spectrum of d(TACGATGAGTA) : d(TACCATCGTA) dissolved in 90% H_2O and 10% D_2O. Intercalation at the bulge site was achieved without the bulged base being ejected from the duplex.

Examples of compounds that specifically intercalate at nucleic acid destabilised sites have been previously reported. In particular, Barton and co-workers have shown that metal complexes ("metalloinsertors") can be designed to preferentially target DNA structures such as mismatched sites, abasic sites and single

base bulges.[17,25,26] These complexes contain a sterically expansive (wide) planar aromatic system (e.g. 5,6-chrysenequinonediimine or benzo[a]-phenazine-5,6-quinonediimine ligands) that stacks into the DNA duplex, but unlike standard intercalating agents, eject a single base or base pair at the binding site.[17] Furthermore, mitoxantrone (a structural analogue of pixantrone) was shown to intercalate between two G•C base pairs that flank an adenine bulge residue in a stem-loop RNA structure.[27] In this case, the drug intercalated from the major groove and the adenine bulge residue was extruded from the duplex.

Bulges are relatively common in RNA, but less so in DNA where they are often an unwanted aberration of the duplex structure.[28] However, there is growing evidence of DNA bulge structures being involved in regulatory processes by serving as recognition points for DNA-binding proteins.[29,30] In particular, bulges can introduce increased flexibility into a segment of DNA that can be specifically recognised by DNA-binding proteins. Although it is unlikely that pixantrone binding to DNA bulges will result in a significant biological affect, due to the low proportion of bulge sites in DNA, it is possible that RNA could be an important target for pixantrone.

In conclusion, the results of this study indicate that the anti-cancer drug pixantrone binds CpA sites equally from either the major or minor groove. This observation may well explain the preferential formaldehyde-activated covalent adducts that are observed at CpA sites. In addition, the results demonstrate that pixantrone preferentially intercalates at an adenine bulge site, compared to duplex DNA, and from the minor groove as opposed to the major groove with duplex CpG sites in DNA.

Acknowledgements

Cell Therapeutics Europe, Italy, is thanked for the pixantrone, while the support of an Australian Research Council Future Fellowship (SMC) is gratefully acknowledged.

References

1. G. Beggiolin, L. Crippa, E. Menta, C. Manzotti, E. Cavalletti, G. Pezzoni, D. Torriani, E. Randisi, R. Cavagnoli, F. Sala, F. C. Giuliani and S. Spinelli, *Tumori* 2001, **87**, 407.
2. L. K. Dawson, D. I. Jodrell, A. Bowman, R. Rye, B. Byrne, A. Bernareggi, G. Camboni and J. F. Smyth, *Eur. J. Cancer*, 2000, **36**, 2353.
3. P. Borchmann, F. Morschhauser, A. Parry, R. Schnell, J. L. Harousseau, C. Gisselbrecht, C. Rudolph, M. Wilhelm, H. G. Derigs, M. Pfreundschuh, G. Camboni and A. Engert, *Haematologica*, 2003, **88**, 888.
4. R. Pettengell, B. Coiffier, G. Narayanan, F. H. de Mendoza, R. Diqumarti, H. Gomez, P. L. Zinzani, G. Schiller, D. Rizzieri, G. Boland, P. Cernohous, L. Wang, C. Kuepfer, I. Gorbatchevsky and J. W. Singer, *Lancet Oncol*. 2012, **13**, 696.
5. T. G. Burke, C. A. Pritsos, A. C. Sartorelli and T. R. Tritton, *Cancer Biochemistry Biophysics*, 1987, **9**, 245.
6. L. A. Hazlehurst, A. P. Krapcho and M. P. Hacker, *Cancer Lett*., 1995, **91**, 115.
7. P. de Isabelle, M. Palumbo, C. Sissi, G. Capranico, N. Carenini, E. Menta, A. Oliva, S. Spinelli, A. P. Keapcho, F. C. Giuliani and F. Zunino, *Mol. Pharmacol*. 1995 **48**, 30.

8. L. A. Hazlehurst, A. P. Krapcho and M. P. Hacker, *Biochem. Pharmacol*., 1995, **50**, 1087.

9. B. J. Evison, O. C. Mansour, E. Menta, D. R. Phillips and S. M. Cutts, *Nucleic Acids Res*., 2007, **35**, 3581.

10. B. J. Evison, F. Chiu, G. Pezzoni, D. R. Phillips, and S. M. Cutts, *Mol. Pharmacol.*, 2008, **74**, 184.

11. B. J. Evison, R. A. Bilardi, F. C. Chiu, G. Pezzoni, D. R. Phillips and S. M. Cutts, *Nucleic Acids Res*., 2009, **37**, 6355.

12. N. Adnan, D. P. Buck, B. J. Evison, S. M. Cutts, D. R. Phillips and J. G. Collins, *Org. Biomol. Chem*., 2010, **8**, 5359.

13. S.-H. Ke and R. M. Wartell, *Biochemistry*, 1995, **34**, 4593.

14. D. M. J. Lilley, *Proc. Natl. Acad. Sci. USA*, 1995, **92**, 7140.

15. R. M. Wadkins, *Curr. Med. Chem.* 2000, **7**, 1.

16. J. W. Nelson and I. Tinoco Jr, *Biochemistry*, 1985, **24**, 6416.

17. B. M. Zeglis, V. C. Pierre and J. K. Barton, *Chem. Commun.* 2007, 4565.

18. J. Caceres-Cortes and A. H.-J. Wang, *Biochemistry*, 1996, **35**, 616.

19. *HyperChem* 7.5, HyperCube, Inc., Gainsville, FL, USA, 2005.

20. R. M. Scheek, R. Boelens, N. Russo, J. H. van Boom and R. Kaptein, *Biochemistry*, 1984, **23**, 1371.

21. J. Feigon, W. Leupin, W. A. Denny and D. R. Kearns, *Biochemistry*, 1983, **22**, 5943.

22. D. J. Patel, L. Shapiro and D. Hare, *J. Biol. Chem*., 1986, **261**, 1223.

23. M. W. Kalnik, D. G. Norman, P. F. Swann and D. J. Patel, *J. Biol. Chem*., 1989, **264**, 3702.

24. M. L. Colgrave, H. E. L. Williams and M. S. Searle, *Angew. Chem. Int. Ed*., 2002, **41**, 4754.

25. R. J. Ernst, H. Song and J. K. Barton, *J. Am. Chem. Soc*., 2009, **131**, 2359.

26. B. M. Zeglis, J. A. Boland and J. K. Barton, *Biochemistry*, 2009, **48**, 839.

27. S. Zheng, Y. Chen, C. P. Donahue, M. S. Wolfe and G. Varani, *Chem. Biol*., 2009, **16,** 557.

28. F. R. Keene, J. A. Smith and J. G. Collins, *Coord. Chem. Rev*. 2009, **253**, 2021

29. D. Payet and A. Tavers, *J. Mol. Biol*., 1997, **266**, 66.

30. S. Chen, A. Gunasekera, X. Zhang, T. A. Kunkel, R. H. Ebright and H. M. Berman, *J. Mol. Biol*. 2001, **314**, 75.